Since January 2020 Elsevier has created a COVID-19 resource centre with free information in English and Mandarin on the novel coronavirus COVID-19. The COVID-19 resource centre is hosted on Elsevier Connect, the company's public news and information website.

Virology 409 (2011) 102–112

Contents lists available at ScienceDirect

Virology

journal homepage: www.elsevier.com/locate/yviro

Early gene expression events in ferrets in response to SARS coronavirus infection versus direct interferon-alpha2b stimulation

Ali Danesh [a,b], Cheryl M. Cameron [a], Alberto J. León [d], Longsi Ran [a], Luoling Xu [a], Yuan Fang [a,b], Alyson A. Kelvin [c,g], Thomas Rowe [a,1], Honglin Chen [d], Yi Guan [d], Colleen B. Jonsson [e], Mark J. Cameron [a], David J. Kelvin [a,d,f,*]

[a] Division of Experimental Therapeutics, Toronto General Research Institute, University Health Network, 101 College Street, Toronto, Ontario, Canada M5G 1L7
[b] Department of Immunology, Faculty of Medicine, University of Toronto, Toronto, ON, Canada M5G 1L7
[c] Immune Diagnostics & Research, IDR , MaRS Centre, 101 College Street, Suite 200, Toronto, ON, Canada M5G 1L7
[d] International Institute of Infection and Immunity, Shantou University Medical College, 22 Xinling Road, Shantou, Guangdong Province, 515031, China
[e] Center for Predictive Medicine, 950 N. Hurstbourne Pkwy, Louisville, KY 40222, USA
[f] Department of Biomedical Sciences, University of Sassari, Sassari, Italy
[g] SaRD, Sardinia Research and Development srl, Porto Conte Ricerche Research Centre, S.P. 55 Porto Conte Capo Caccia km 8,400, Loc. Tramariglio, 07041, Alghero (SS), Italy

ARTICLE INFO

Article history:
Received 25 February 2010
Returned to author for revision
23 August 2010
Accepted 1 October 2010
Available online 28 October 2010

Keywords:
Ferret
Gene expression
SARS
Interferon

ABSTRACT

Type I interferons (IFNs) are essential to the clearance of viral diseases, however, a clear distinction between genes upregulated by direct virus–cell interactions and genes upregulated by secondary IFN production has not been made. Here, we investigated differential gene regulation in ferrets upon subcutaneous administration of IFN-α2b and during SARS-CoV infection. *In vivo* experiments revealed that IFN-α2b causes STAT1 phosphorylation and upregulation of abundant IFN response genes (IRGs), chemokine receptors, and other genes that participate in phagocytosis and leukocyte transendothelial migration. During infection with SARS-CoV not only a variety of IRGs were upregulated, but also a significantly broader range of genes involved in cell migration and inflammation. This work allowed dissection of several molecular signatures present during SARS-CoV which are part of a robust IFN antiviral response. These signatures can be useful markers to evaluate the status of IFN responses during a viral infection and specific features of different viruses.

Introduction

Viral respiratory infections are a major worldwide cause of morbidity and mortality (Kolling et al., 2001; Thompson et al., 2003). Emerging viral threats, such as the severe acute respiratory syndrome coronavirus (SARS-CoV), avian influenza H5N1 and pandemic influenza H1N1 virus are well poised to cause epidemics or pandemics that could be socially and economically disastrous (Dushoff et al., 2006; Weiss and McMichael, 2004; Dawood et al., 2009).

For decades, ferrets have been used for the investigation of influenza infection since they are susceptible to influenza viruses (Hull and Loosli, 1951). More recently, ferrets have also been shown to be a good model of human SARS-CoV infection (Martina et al., 2003). We have previously characterized ferret cytokine and chemokine genes as well as have developed immunological assays for evaluating the ferret immune system following SARS and influenza infection (Cameron et al., 2008; Danesh et al., 2008; Ochi et al., 2008).

Ligation of the interferon (IFN) alpha receptors 1 and 2 (IFNAR1 and IFNAR2) with IFN-α induces IFN signaling pathways and promotes IFN gene induction. Formation of the signal transducer and activator of transcriptions 1 and 2 (STAT1–STAT2) heterodimer occurs following the phosphorylation of Janus kinase 1 (JAK1) and tyrosine kinase 2 (Tyk2) that are associated with IFNAR2 and IFNAR1, respectively (Marijanovic et al., 2007). These two kinases phosphorylate STAT1 and STAT2, which together form a complex with interferon regulatory factor 9 (IRF9) (Takaoka and Yanai, 2006). The interferon stimulatory factor 3 complex (ISGF3) binds to interferon-stimulated response element (ISRE) and activates transcription of IFN-α inducible genes, including 2'–5' oligoadenylate synthase 1 (OAS1), myxovirus resistance 1 (MX1), interferon stimulated gene 15 (ISG15) and many other IFN-response genes (IRGs) (Uddin and Platanias, 2004).

IFN-α stimulation ultimately promotes a cellular antiviral state which is hallmarked by the upregulation of IRGs (Chevaliez and Pawlotsky, 2007). Although IFN signaling gene upregulation during viral infection has been the subject of previous reports, there is little information regarding the host immune responses directly induced by viruses versus those that are upregulated due to secondary IFN stimulation (Chelbi-Alix

* Corresponding author. Division of Immunology, International Institute of Infection and Immunity, Shantou University Medical College, 22 Xinling Road, Shantou, Guangdong, China, 515041. Fax: +86 754 88573991.
E-mail address: dkelvin@uhnres.utoronto.ca (D.J. Kelvin).
[1] Present address: Centers for Disease Control and Prevention, Influenza Division, 1600 Clifton Road, MS:G-16, Atlanta, GA 30333, USA.

0042-6822/$ – see front matter © 2010 Elsevier Inc. All rights reserved.
doi:10.1016/j.virol.2010.10.002

and Wietzerbin, 2007; Haagmans et al., 2004; Loutfy et al., 2003; Cameron et al., 2007). Here we used our previously described ferret model (Chu et al., 2008) to identify genes that were regulated by SARS-CoV infection compared to IFN-α2b stimulation in the ferret model to elucidate immune responses during viral infection. We examined the phosphorylation status of signaling molecules in IFN-α2b-stimulated peripheral blood mononuclear cells (PBMCs). We also analyzed the *in vivo* gene expression profiles of ferret PBMCs and lung necropsies following IFN-α2b injection during the time course. Evaluation of gene expression patterns in PBMCs and lung necropsies of SARS-CoV-infected ferrets led us to the identification of 7 upregulated IRGs that also were upregulated in response to IFN-α2b injection. Our findings in ferrets suggested IFN-α2b injection and SARS-CoV infection led to similar as well as unique gene expression signatures in a global point of view. Increased knowledge of the interaction of these gene expression signatures may improve our understanding of the immune system of ferrets as a preferred animal model of severe respiratory viral illnesses.

Results

IFN-α2b stimulation and SARS-CoV infection induced STAT1 phosphorylation and increased the expression levels of IRGs

We first investigated the phosphorylation of the IFN-α receptor downstream signaling molecule STAT1 to determine the signaling potential of IFN-α2b in ferrets. The phosphorylation status of STAT1 was evaluated using phosphorylated amino acid specific monoclonal antibody for flow cytometry analysis that cross-reacted with the phosphorylated ferret protein. PBMCs demonstrated a significant STAT1 phosphorylation response 15 min post-stimulation with IFN-α2b *in vitro* compared to the control stimulated with PBS alone (Supplementary Fig. 1).

Since STAT1 phosphorylation was observed *in vitro*, we then determined whether IFN-α2b could activate STAT1 *in vivo*. Four ferrets were subcutaneously injected with 1 μg/kg IFN-α2b and peripheral blood samples were taken at 0, 3 and 6 h post-stimulation for flow cytometry examination. By 3 h, samples extracted from all ferrets demonstrated significant STAT1 phosphorylation in the PBMCs. Control ferrets injected with PBS did not demonstrate marked STAT1 phosphorylation at any time point. The STAT1 average mean fluorescent intensity (MFI) of the IFN-α2b-injected group was significantly increased compared to the average of its control group ($P<0.01$) (Fig. 1A). These results indicated that STAT1 was also inducible by IFN-α2b *in vivo*.

IFN signaling is critical to successful antiviral responses during infection (Haller et al., 2007). Therefore, we next investigated the phosphorylation status of STAT1 following SARS-CoV infection. We infected ferrets with SARS-CoV or PBS control and measured the phosphorylation of STAT1 by flow cytometry. Three ferrets infected with SARS-CoV demonstrated significant STAT1 phosphorylation in PBMCs post-infection with a maximum peak at day 3 ($P<0.01$). Control ferrets mock-infected with PBS did not demonstrate significant STAT1 phosphorylation at any time point (Fig. 1B).

Since STAT1 was phosphorylated following SARS-CoV infection and IFN-α2b injection, we investigated select IRG expression by qRT-PCR following *in vitro* stimulation of ferret peripheral whole blood with IFN-α2b. *In vitro* stimulation with IFN-α2b led to significant upregulation of STAT1 and several IRGs such as MX1, OAS1, ISG15, ISG20, IRF7 and interferon-induced protein 35 (IFI35). As expected, activation of IFN-α receptor signaling therefore initiated transcriptional activation of interferon response genes (Supplementary Fig. 2).

Microarray analysis of IFN-α2b injection or SARS-CoV infection in ferret peripheral blood

We then assessed genome-wide gene expression following *in vivo* IFN-α2b administration in ferrets. Ferrets were subcutaneously injected with PBS (control) or IFN-α2b and blood samples were drawn for RNA isolation 1 and 2 days after injection. Without a commercially available ferret microarray, the RNA was then used for microarray analysis on the Affymetrix GeneChip Canine Genome 2.0 Array (see Materials and methods), because ferret genes show a high degree of homology with canine genes as we have previously established (Cameron et al., 2008; Rowe et al., 2010; Fang et al.,

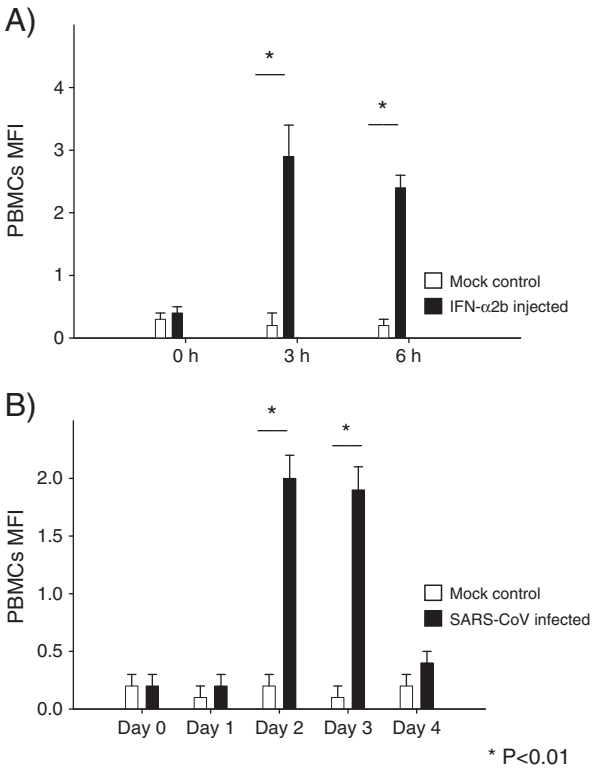

Fig. 1. *In vivo* phosphorylation of STAT1 in ferret peripheral blood mononuclear cells. (A) *In vivo* stimulation with IFN-α2b; the STAT1 average mean fluorescent intensities (MFI) of IFN-α2b-injected ($n=4$) and control ($n=4$) groups were measured by flow cytometry during the time course (X axis) in the PBMC gate. The Y axis indicates the Δ MFI between STAT1 phosphorylation and isotype control. White bars: Control group, black bars IFN-a2b-injected group. $P<0.01$, using Student t test. (B) *In vivo* infection with SARS-CoV; the STAT1 average MFI in PBMCs of 3 SARS-CoV-infected ferrets (black bars) versus 3 mock controls (white bars) during the time course ($P<0.01$). Bars are representative averages of Δ MFI between STAT1 phosphorylation and isotype control.

Table 1
Summary of differentially regulated genes in top functional groups during the time course in IFN-α2b-injected or SARS-CoV-infected ferrets.

	IFN-a2b				SARS-CoV		
	Day 1		Day 2		Day 1	Day 2	
	BL	LG	BL	LG	LG	BL	LG
Total upregulated genes	716	82	2717	512	4222	138	1014
Total downregulated genes	51	147	1230	550	1248	414	894
Cellular process ↑	440	44	1581	266	2180	69	542
Cellular process ↓	15	83	577	318	570	229	427
Metabolic process ↑	328	30	1212	175	1573	52	369
Metabolic process ↓	8	58	383	247	392	188	297
Intracellular signaling cascade ↑	50	3	205	40	271	12	63
Intracellular signaling cascade ↓	2	11	81	0	80	29	60
Cell cycle ↑	48	6	160	23	178	6	45
Cell cycle ↓	0	11	36	44	38	30	29
Immune response ↑	32	6	82	18	125	9	44
Immune response ↓	0	2	32	0	39	7	29

Number of regulated genes in different functional categories with at least 1.5-fold change and a significant t-test of $P<0.05$ (↑ upregulated, ↓ downregulated).

2010) (Supplementary Table 1). The peripheral blood gene expression data from IFN-α2b-injected group were normalized to the control group. The *t*-test analyses showed the highest number of significant changes occurred at day 2, with a total of 2717 upregulated and 1230 downregulated genes in peripheral blood of the IFN-α2b-injected ferrets (Table 1). A threshold of at least 1.5 fold-change and a *P* value for the *t*-tests of less than 0.05 were chosen. The peak upregulation of a cluster of IRGs, including MX1, OAS1, OAS2, ISG15, IFI44 and ubiquitin specific protein 18 (USP18), occurred at day 1, while peak upregulation of IRGs such as JAK1, JAK2, protein inhibitor of activated STAT1 (PIAS1) IRF1, interferon-γ receptor 1 (IFNGR1), and eukaryotic translation initiation factor 2-α kinase 2 (EIF2AK2) occurred at day 2 post-injection (Fig. 2A and Supplementary Table 2).

After assessing the large scale gene expression profile following ferret *in vivo* IFN-α2b stimulation, we validated the expression of selected IRGs by qRT-PCR according to the availability of the ferret specific primers. We found STAT1 and IRGs such as MX1, OAS1 and ISG15 were significantly upregulated in ferrets injected with IFN-α2b

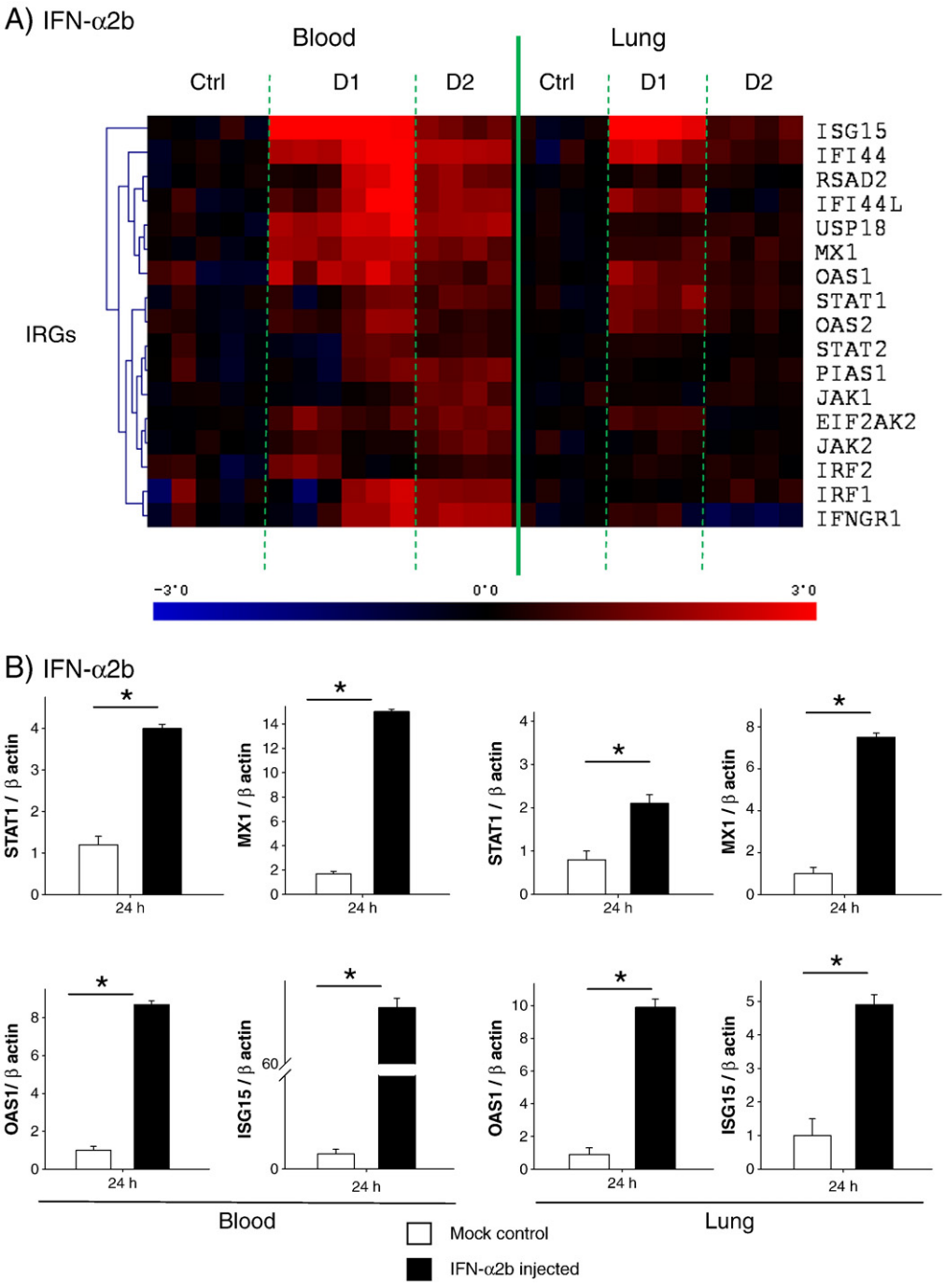

Fig. 2. Microarray and qRT-PCR analysis of IRG expression in peripheral blood and lung necropsies of ferrets injected with IFN-α2b or infected with SARS-CoV *in vivo* during the time course. (A) Ferrets were injected with IFN-α2b or with PBS. Whole blood or lung necropsies were collected at day 1 and day 2. mRNA was purified, converted to cRNA and ran on the Affymetrix Canine gene chip II. Hierarchal microarray EDGE analysis demonstrated a cluster of IRGs, which were significantly upregulated (red color). (B) Upregulation of IRGs was confirmed at peak time-points with qRT-PCR, where ferret specific primers were available. White and black bars are the mean gene expression level of control and injected ferrets respectively, normalized to β actin. (C) Differential upregulation of IRGs observed following the microarray analysis of blood and lung necropcies of ferrets infected with SARS-CoV. (D) Upregulation of 4 IRGs was confirmed by qRT-PCR.

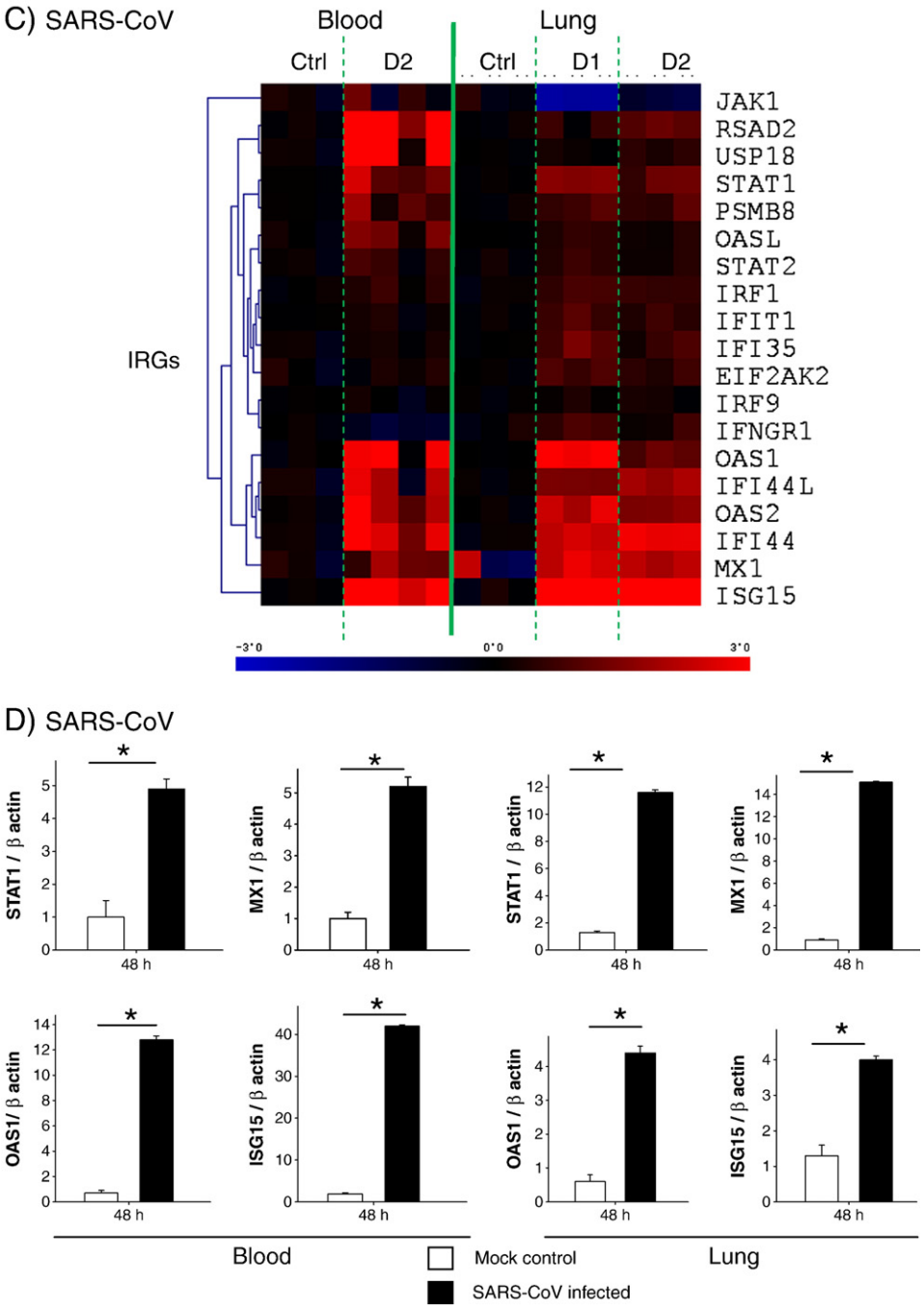

Fig. 2 (*continued*).

compared to the controls (Fig. 2B). The lack of ferret sequences for other IRGs prevented us from confirming the upregulation of these genes.

To determine if STAT1 phosphorylation was correlated with IRG activation in our ferret animal model of SARS-CoV infection (Chu et al., 2008), we went on to analyze host gene expression following SARS-CoV infection. The gene expression data at day 2 post-infection with SARS-CoV was normalized to the mock control dataset. Unfortunately, blood samples from day 1 post-infection did not meet minimal RNA quality for microarray analysis, preventing us from performing a time-course study on the peripheral blood. There were 138 upregulated and 414 downregulated genes ($P<0.05$, >1.5 fold change) as ascertained by *t*-test analysis at day 2 post-infection (Table 1). IRGs, including STAT1, MX1, OAS1, OAS2, ISG15, IFI44, suppressor of cytokine signaling 1 (SOCS1), radical S-adenosyl methionine domain containing 2 (RSAD2), USP18 and OAS ligand (OASL) were significantly upregulated (Fig. 2C and Supplementary Table 2). The upregulation of STAT1, MX1, OAS1 and ISG15 were validated with qRT-PCR (Fig. 2D). These gene expression and STAT1 phosphorylation findings suggested that robust IFN responses were activated following SARS-CoV infection 2 days post-infection.

Interferon canonical pathway analysis confirmed the similarities between the expression patterns of IRGs at day 2. STAT1, MX1, OAS1, USP18, RSAD2, ISG15 and IFI44 were upregulated in the peripheral blood of IFN-α2b-injected and SARS-CoV-infected ferrets. In contrast, OASL, OAS2 and SOCS1 were upregulated during SARS-CoV infection alone (Fig. 3A).

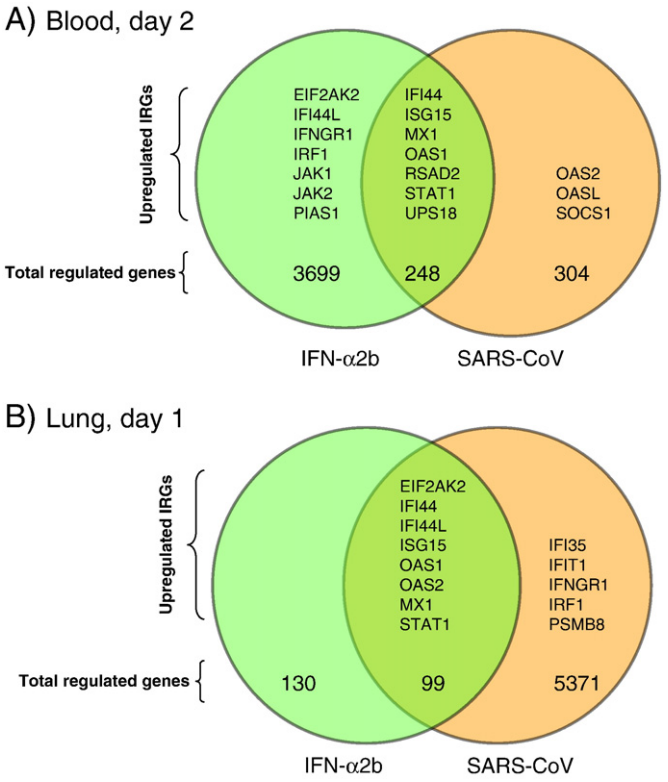

Fig. 3. Intersect analysis of IRGs expression in blood and lung tissue from IFN-α2b-injected and SARS-CoV-infected ferrets. Venn diagrams are representative of IRGs upregulation and indicate the total number of regulated genes. The time points were chosen according to the highest expression levels of IRGs. For more information, refer to Supplementary table 2.

Microarray analysis of IFN-α2b injection or SARS-CoV infection in ferret lungs

Since SARS-CoV infection causes severe lung pathology we went on to compare and contrast the genes upregulated by IFN-α2b stimulation and SARS-CoV infection in the lungs of ferrets. Microarray analysis was performed on lung necropsies of IFN-α2b-injected ferrets compared to controls. The peak gene expression occurred at day 2 with a total of 512 upregulated and 550 downregulated ($P<0.05$) genes (Table 1). Interestingly, the strongest upregulation of several IRGs, such as STAT1, MX1, OAS1, OAS2, ISG15, IFI44, IFI44 ligand (IFI44L) and EIF2AK2, occurred on day 1 (Fig. 2A and Supplementary Table 1). There was a marked increase in the total number of regulated genes from lung necropsies of SARS-CoV-infected ferrets compared to lungs from IFN-α2b-stimulated ferrets (Table 1). The SARS-CoV infected ferrets had a peak in gene expression at day 1 with 4222 upregulated versus 1248 downregulated genes ($P<0.05$). Both the number of upregulated IRGs and the expression levels peaked at day 1, including STAT1, MX1, OAS1, OAS2, ISG15, IRF1, interferon-induced protein with tetratricopeptide repeats 1(IFIT1), IFI35, IFI44, IFI44L, proteasome subunit multifunctional beta 8 (PSMB8), EIF2AK2 and IFNRG1. JAK1 was the only IRG that was downregulated at day 1 (Fig. 2C). The upregulation of STAT1, MX1, OAS1 and ISG15 was validated with qRT-PCR on lung necropsies of ferrets injected with IFN-α2b or infected with SARS-CoV (Fig. 2D). The comparison of microarray results between the lung tissue of IFN-α2b and SARS-CoV ferrets at day 1 revealed commonalities in the expression patterns of most IRGs. STAT1, MX1, OAS1, OAS2, ISG15, IFI44, IFI44L and EIF2AK2 were among the overlapping genes (Fig. 3B).

Pathway and functional group differential gene expression patterns

To further model the pathways involved in the host response to SARS-CoV and the direct effects of IFN-α2b administration, functional analysis of the regulated genes was performed using Ingenuity Pathway Analysis software. For each experimental group, genes showing changes in their expression levels were mapped into high-level Gene Ontology categories: cellular process, metabolic process, intracellular signaling cascade, cell cycle and immune response (Table 1). The number of genes present in each functional category is representative of the level of biological activity in each experimental group with respect to the controls. Analysis of the IFN signaling canonical pathway showed the upregulation of STAT1, MX1, OAS1, OAS2, ISG15 and IFI44 in lung necropsies of IFN-α2b injected and SARS-CoV infected ferrets (Fig. 4).

Functional classification of upregulated genes showed that IFN-α2b induces increased expression of phagocytosis-related genes, such as Fc fragment of IgG, high affinity Ia, receptor CD64 (FCGR1A) and dynamin 1-like (DNM1L), leukocyte transendothelial migration genes, such as integrins beta 1 and 2 (ITGB1 and ITGB2), and upregulation of chemokine receptors, chemokine C-C motif receptors 3, 7 and 9 (CCR3, CCR7, CCR9) and chemokine C-X-C motif receptor 4 (CXCR4) (Supplementary Table 3). These results suggest that IFN-α2b is able to activate specific functions of the leukocyte responses in blood samples after exposure.

The lungs of ferrets infected with SARS-CoV showed broader immune responses than IFN-α2b-injected ferrets, as demonstrated by the higher number of regulated genes in several functional categories related to the activation of the immune responses, including: complement and coagulation, cell adhesion molecules and leukocyte activation (Fig. 5).

Discussion

Type I IFNs are a critical component of the innate immune response during viral infections. The function of many downstream genes has been studied in-depth, however, it is likely that the presence of the virus and subsequent TLR-mediated signaling are required to deploy full IRG-mediated antiviral activity (Bosinger et al., 2009). In this study we investigated the gene signatures induced following subcutaneous administration of IFN-α2b in ferrets. We also analyzed the signaling pathways during an infection with SARS-CoV, and by means of comparative analysis we profiled IFN gene responses in the context of a respiratory infection. We used an experimental model of infection with SARS-CoV in ferrets, which causes mild symptoms without mortality. The pathological features of this model were previously published (Chu et al., 2008) and a summary of the clinical information can be found in the supplementary information (Supplementary Table 4).

We assessed the capacity of subcutaneous administration of IFN-α2b to activate antiviral responses in ferrets. The activation levels of several intracellular signaling proteins were studied by using phospho-specific antibodies and subsequent FACS analysis. STAT1 plays a key role downstream of IFN signaling while STAT3 and STAT5 are thought to be involved at a lesser extent, and/or weak participation of STAT4, mitogen activated protein kinase 38 (p38) and Extracellular Signal-Regulated Kinase (ERK) (Li et al., 2007). *In vitro* incubation of ferret PBMCs with IFN-α2b led to strong phosphorylation of STAT1, weak phosphorylation of STAT3 and

Fig. 4. IRG pathway analyses of microarray datasets in lung necropsies of IFN-α2b-injected and SARS-CoV-infected ferrets. Ingenuity pathway analyses indicated similar patterns of IRGs upregulation, downstream of STAT1 signaling pathway in lung tissue from ferrets (A) injected with IFN-α2b and (B) infected with SARS-CoV.

A)

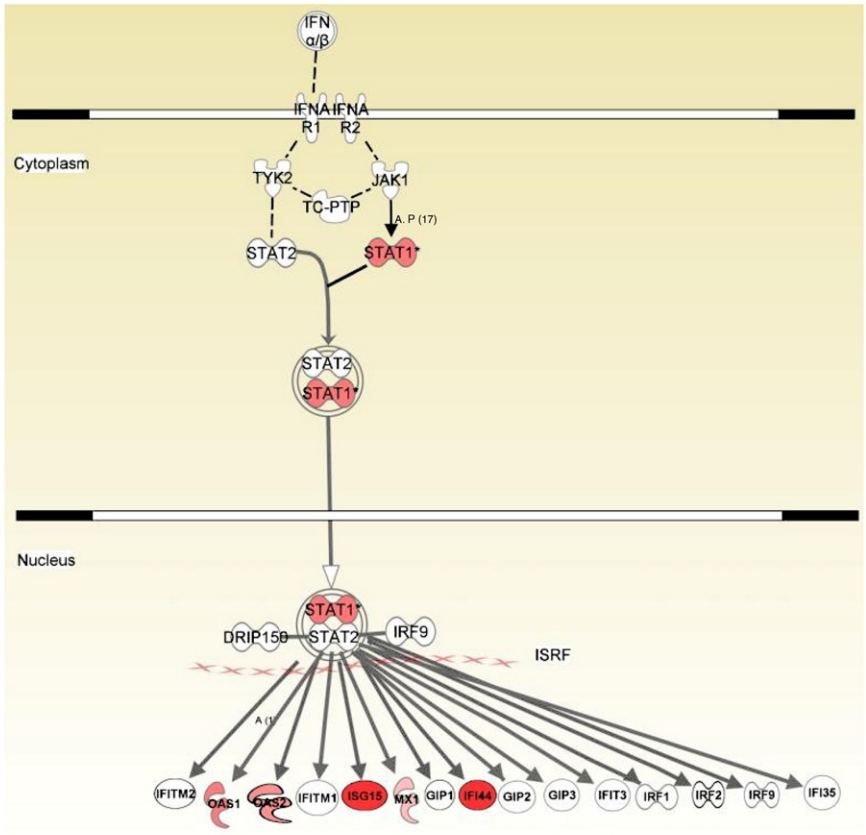

IFN-α2b injected ferrets

B)

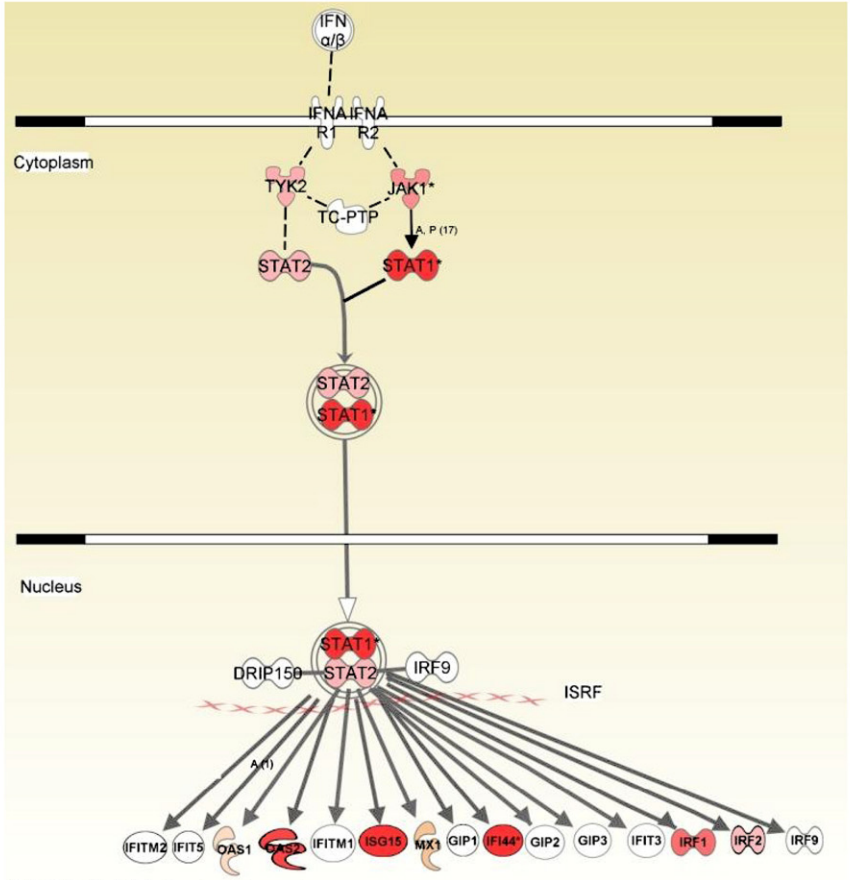

SARS CoV infected ferrets

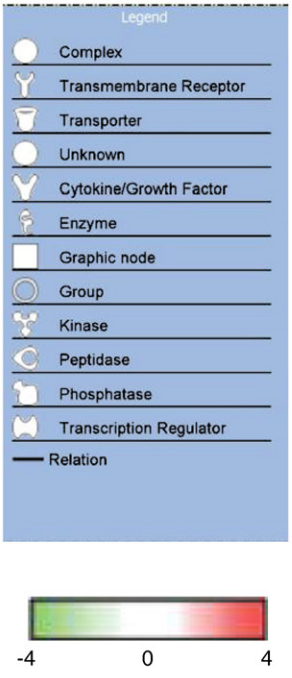

STAT5 and no phosphorylation of STAT4, p38 and ERK. Furthermore, the activation of the STAT1 signaling pathway *in vitro* was confirmed at the mRNA level with the presence of many downstream IRGs, including MX1, OAS1, OAS2, ISG15, and IFI44. The *in vivo* effects of IFN-α2b were also investigated. STAT1 showed increased phosphorylation levels in the peripheral blood at early hours post-injection, while STAT3 and STAT5 remained unchanged. Moreover, we did not observe mRNA gene expression of interleukin 8 (IL-8) and Suppressor of Cytokine Signaling 3 (SOCS3) at the mRNA level (data not shown), suggesting that STAT3 (Gharavi et al., 2007) and STAT5 (Barclay et al., 2007), respectively, do not participate *in vivo* in response to IFN-α2b.

The global numbers of regulated genes found in the microarray results constitute good estimators of the intensity of the host response at different time-points. *In vivo* effects of IFN-α2b can be observed 24 h after the injection and their peak is reached 48 h post-injection. IRGs are markedly increased in both blood and lung tissue, however the responses in the blood show greater breadth and magnitude as compared with the responses observed in lung tissue (Supplementary Table 2). This suggests that the administration protocol of IFN-α2b used in this study is only capable of inducing a limited activation in lung tissue. Therefore, alternative protocols including direct administration of IFN-α2b into the respiratory tract or subcutaneous administration at higher doses should be explored in order to achieve stronger antiviral responses at the infection sites. Gene expression during SARS-CoV infection, on the other hand, shows the presence of strong antiviral and inflammatory responses in the lungs 24 h post-infection, fading on day 2 post-infection in both blood and lung tissue.

As expected, IFN-α2b stimulates the increased expression of a variety of IRGs that play a central role in the clearance of viral infections, including MX1, OAS1, OAS2 and ISG15. They exert their effects through different mechanisms of action, such as direct targeting of viral entry, inhibition of protein synthesis or degradation of viral RNA. MX1 is a dynamin-like large guanosine triphosphatase (GTPase), which has antiviral activity against a wide range of RNA viruses. The antiviral activity of MX1 is effective at the early stages of the viral cycle in the nucleus or cytoplasm (Haller et al., 2007). OAS is an adenylate synthetase, which uses adenosine triphosphate to synthesize 2',5'-oligoadenylates. The latter activates latent RNase L that is involved in the degradation of viral RNA (Bonnevie-Nielsen et al., 2005). ISG15 is a ubiquitin-like enzyme that covalently conjugates to a large number of cellular proteins; however this does not usually lead to protein degradation. In the case of HIV-1, ISG15 inhibits the release of virions (Okumura et al., 2006).

Upregulation of similar sets of IRGs by SARS-CoV and IFN-α2b were observed, including 7 IRGs (STAT1, ISG15, MX1, OAS1, OAS2, IFI44 and IFI44L) in the peripheral blood and lung tissue of both groups. In contrast, several IRGs, including IFI35, IFIT1 and PSMB8, were only upregulated in the lungs during SARS-CoV infection. These results suggest that the expression of certain IRGs lie beyond the direct control of IFN-α2b, and additional signals such as activation of TLR-signaling by viral components are probably required to assemble a fully functional antiviral response.

Although the induction of IRGs by IFN-α2b is the hallmark feature of IFN responses, a full understanding of the biological effects of antiviral IFNs requires a comprehensive study of the additional functional responses triggered by IFN-α2b. In the blood of ferrets injected with IFN-α2b, the upregulation of genes that participate in glycolysis-gluconeogenesis (e.g. acyl-CoA synthetases and lactate dehydrogenases) (Supplementary Table 3) are indicators of higher levels of metabolic activity. Moreover, IFN also induces the expression of genes related with apoptosis (e.g. caspases and TNFSF10) and cell cycle (e.g. cyclins and SMAD family members). It is unclear whether IFN-α2b alone is capable of inducing apoptosis and/or cell replication *in vivo*, however, the upregulation of these genes may indicate that PBMCs are now more responsive to signals capable of triggering cell cycle events. Upregulation of chemokine receptors, such as CCR3, CCR7, CCR9 and CXCR4 may indicate that IFN-α2b can increase the responsiveness of PBMCs to locally produced chemokines. Likewise, increased levels of genes that are involved in leukocyte transendothelial migration and Fc-gamma receptor-mediated phagocytosis (Supplementary Table 3) suggest that IFN-α2b enhances leukocyte responses (Corssmit et al., 1997). Interestingly, a number of genes that are part to the Wnt signaling pathway were found to be upregulated (Supplementary Table 3). This indicates that *in vivo* administration of IFN-α2b also has effects over lymphocyte maturation and differentiation (Staal et al., 2008).

The lungs of ferrets infected with SARS-CoV show the upregulation of a broader variety of genes, as compared with IFN-α2b administration, and depicts a more complex biological environment dominated by the antiviral responses, leukocyte infiltration and other inflammatory responses (Fig. 5B). A number of chemokine ligands, such as chemokine C-C motif ligand 2 (CCL2), CCL4, CCL14, CCL19 and CCL25, and cell adhesion molecules, such as activated leukocyte cell adhesion molecule (ALCAM) and intercellular adhesion molecule 1 (ICAM1) are upregulated during SARS-CoV infection, but these were not induced by the administration of IFN-α2b (Fig. 5A and Supplementary Table 3). SARS-CoV also induced the upregulation of genes of the complement system such as complement component 3 (C3) and complement factor B (CFB) (Fig. 5B). Taken together, these results depict how IRGs and other arms of the innate immune responses are capable of resolving the respiratory infection caused by SARS-CoV infection.

Previously, gene regulation has been investigated using microarray analysis with the intent on revealing molecular pathways imperative to H1N1 infection (Shapira et al., 2009). Here we investigated gene regulation of SARS-CoV infected and IFN-α2b injected ferrets. Microarray analysis was conducted on RNA from lungs and blood on day 1 and day 2. The number of upregulated genes was quantified and compared to the number of downregulated genes for each sample type. The number of downregulated genes was greater than upregulated genes in the day 1 IFN-α2b lungs and in the day 2 SARS-CoV infected blood samples. To expose the molecular signature of this finding we then broke down the genes from each group into their respective functional pathways: cellular process, metabolic process, intracellular signaling cascade, cell cycle, and immune response. Interestingly, we found that for every functional pathway the day 1 IFN-α2b-injected lungs had more downregulated genes than upregulated genes (except the immune response) where blood samples from the same animals had the opposite trend of more upregulated genes. Furthermore, the SARS-CoV-infected animals had the opposite trend where day 1 lungs had more upregulated genes and in the blood of day 2 there were more downregulated genes. These findings may be indicative of the activity of the stimulant IFN-α2b compared to SARS-CoV. Moreover, the difference in the number of genes regulated shows that IFN-α2b and SARS-CoV have different spatial stimulation which may be an important finding when determining the therapeutic efficacy of IFN-α2b. It is possible that the increase in gene expression in the blood samples following IFN-α2b injection is indicative of activation of systemic immunity where the SARS-CoV infection had an increase of lung gene expression signifying possible local inflammation.

Type I IFNs play a critical role during antiviral responses, however their functions *in vivo* have not yet been fully resolved. Additional research is required to define the optimal IRGs profile that is present during successfully cleared viral infections. Moreover, fine tuning of the IRGs responses may achieve more prolonged and wider protection by therapeutic agents such as attenuated vaccines against respiratory viruses.

Materials and methods

Ferrets

Male, 1 kg, 6-month-old ferrets (*Mustela putorius furo*) were purchased from Marshall Farms Inc. (Oak Park, IL) and housed at

the Toronto General Research Institute animal facility (Toronto, Canada) or at Southern Research Institute (Birmingham, AL, USA). Ferrets were quarantined and monitored 5 days prior to tissue and blood collection. The ferrets' diet was based on a low fat/high protein regimen as recommended by Marshal Farms. Animal protocols were approved and monitored by the Animal Care Committee of the University Health Network or of the Southern research Institute.

In vitro blood stimulation with IFN-α2b

Whole blood was drawn from 4 ferrets and diluted ¼ with cell culture media (Invitrogen, CA). Two ml of diluted blood from 4 animals was stimulated with 0.001 μg/ml IFN-α2b (pegylated IFN-α2b, Schering-Plough, Pointe-Claire, Canada) in separate wells and incubated at 37 °C (5% CO_2) for 1 and 3 h. PBS was added to 3 control wells. The cultured blood was then harvested and injected to PaxGene tubes. RNA was purified according to manufacturer's protocol (Invitrogen, CA). One ml of blood stimulated with IFN-α2b and or PBS was also added to 10 ml Lyse/Fix buffer (BD Biosciences, USA) for evaluation of phosphorylation status of signaling molecules at 0, 15, 30, 45, 60, 75 and 90 min, using PhosFlow antibodies (BD Biosciences, USA).

In vivo injection of ferrets with IFN-α2b

Subcutaneous injections of 1 ml of PBS (control) or 1 μg/ml of IFN-α2b were performed on the back of each ferret. Two ml of blood was collected directly into PaxGene tubes. One gram of the lung necropsy was added to TRIzol® reagent (Invitrogen CA). Collected blood and lung tissues were used for RNA isolation according to the manufacturer's protocol and used for microarray, and quantitative real-time PCR analysis. One ml blood was added to Lyse/Fix buffer (BD Biosciences, San Jose, CA) for analysis of the signaling molecule phosphorylation status.

In vivo infection of ferrets with SARS-CoV

Ferrets were infected with SARS-CoV in the Animal Biohazard Safety Level 3 (ABSL3) facility at Southern Research Institute (Birmingham, AL, USA), in accordance with the approved protocols. Three male ferrets, weighing approximately 800–1000 g, were infected intranasally with 10^3 $TCID_{50}$ SARS-CoV TOR2 strain (isolated from a patient in Toronto and sequenced at CDC, Vancouver, BC) in 1 mL PBS. An additional 3 animals were mock-infected with 1 mL PBS.

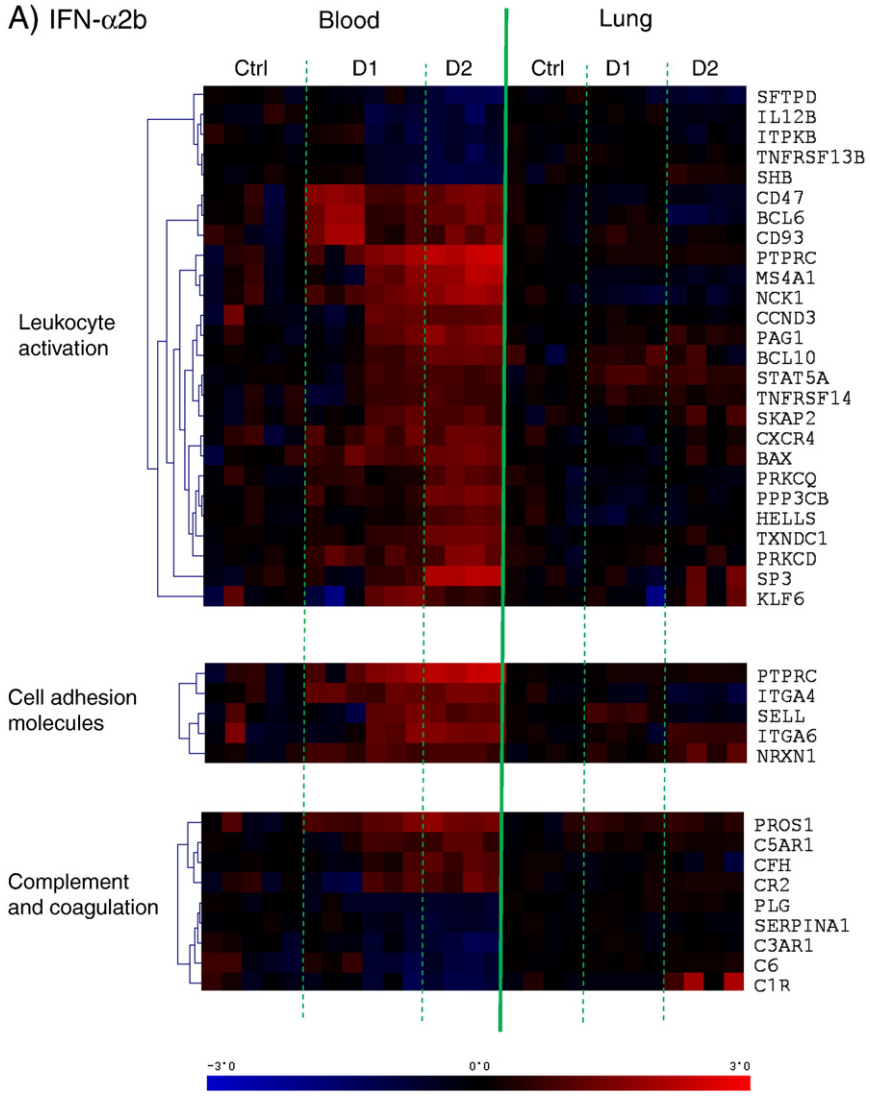

Fig. 5. Microarray analysis of immune response pathways in peripheral blood and lung necropsies of ferrets injected with IFN-α2b or infected with SARS-CoV *in vivo* during the time course. Whole blood or lung necropsies were collected at different time-points. mRNA was purified and used for microarray EDGE analysis. Three immune pathways that play key roles in early immune responses ("Leukocyte activation," "cell adhesion molecules" and "complement and coagulation") were used to identify similarities and differences. Red and blue colors are representative of upregulation and downregulation, respectively. (A) IFN-α2b-injected ferrets. (B) SARS-CoV-infected group.

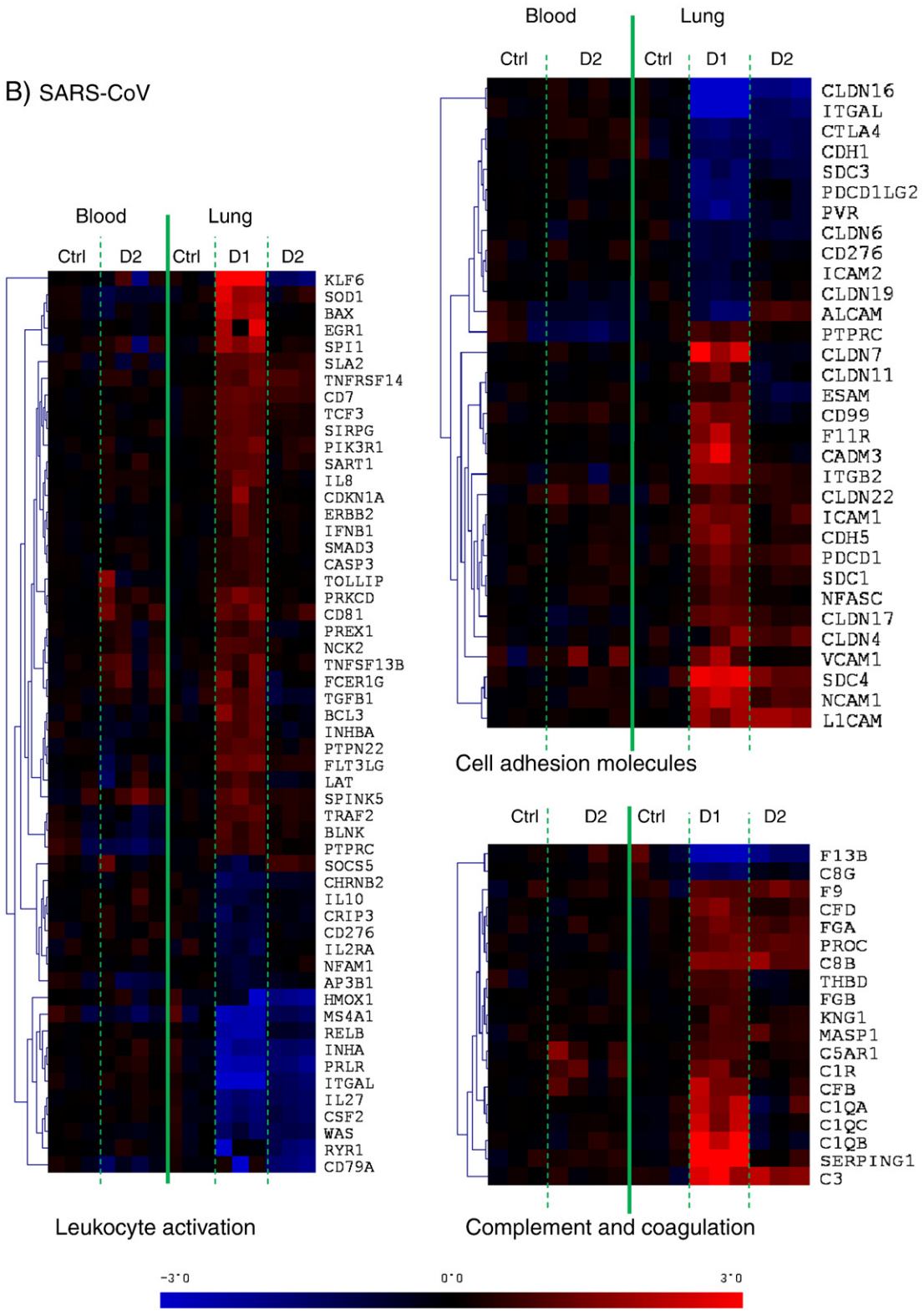

Fig. 5 (*continued*).

Animals were anesthetized and blood and lung necropsies were collected for RNA purification. Infection of ferrets with the above mentioned dose results in weight loss, decreased activity, temperature increase and histology lesions with no mortality during the disease course (Chu et al., 2008). A summary of natural history of ferrets infected with SARS-CoV has been provided as Supplementary Table 4.

Intracellular staining

One ml of *in vitro*-stimulated blood with IFN-α2b or PBS and/or 1 ml of blood drawn from the IFN-α2b or PBS injected ferrets and/or 1 ml blood from infected ferrets with SARS-CoV or mock controls (*in vivo*) was added to 10 ml Lyse/Fix buffer (BD Biosciences, USA) and

incubated in a 37 °C water bath for 10 min. Tubes were then centrifuged at 300*g* for 5 min and the cells were washed twice with cold PBS. One ml Perm III (BD Biosciences, USA) was added to each tube and the tube was incubated on ice for 20 min to permeabilize cells for intracellular staining. Cells were washed with Perm/Wash (BD Biosciences, USA) and 10^6 cells were added to each tube for flow cytometry. Twenty microliters of phosphorylated (P)-STAT1, P-STAT3, P-STAT4, P-STAT5, P-p38 and P-ERK antibodies conjugated with Alexa-Fluor 488 was added to separate tubes (BD Biosciences, USA). Matched isotype control was added to one tube as a negative control. Tubes were incubated at room temperature in the dark for 30 min. Cells were washed with cold Perm wash (BD Biosciences, USA) and fixed with 2% paraformaldehyde in PBS. Twenty thousand events were acquired with a BD FACSCalibur (BD Biosciences, USA) and data were analyzed, using FlowJo software (Tree Star Inc., USA).

Cloning and sequencing of ferret-specific genes

Cloning and sequencing was performed as described previously (Danesh et al., 2008). Briefly, purified RNA was reverse transcribed to cDNA using Invitrogen RT-kits (Invitrogen, Carlsbad, CA). Gene-specific degenerate primers were designed based on multiple gene sequence alignment analysis of several species using ClustalW (1.83) and then used to clone the cDNAs for each gene. Standard PCRs were performed and specific bands were gel-purified (Qiagen, Mississauga, Canada) and cloned into the pCR 2.1-TOPO vector (Invitrogen, Carlsbad, USA). Sequences of positive clones were confirmed using an ABI 3730XL DNA analyzer (Applied Biosystems, Foster City, CA). The identification of genes was performed using Basic Local Alignment Search Tool (BLAST) analyses against National Centre for Biotechnology Information (NCBI) database.

Gene accession numbers

STAT1 (EU835493), STAT2 (EU835988), MX1 (EU835483), OAS1 (EU835484), ISG15 (EU835986), ISG20 (EU835990), IRF7 (EU835985), IFI35 (EU835487), PKR (EU835989), P52RIPK (EU835488), CXCL8 (EU835489), SOCS3 (EU835987).

Quantitative Real-Time PCR (qRT-PCR)

The following components were added to the reaction mixture plus cDNA to a total volume of 10 μL in distilled water: 0.2 μl cDNA, 250 nmol forward gene-specific primer, 250 nmol reverse gene-specific primer and 5 μL Cyber Green (Applied Biosystems, Foster City, CA). For every experiment, each reaction was performed in triplicate. An ABI 7900 Sequence Detection System (Applied Biosystems, Foster City, CA) was used for amplification. Initial denaturation was 15 min at 95 °C, followed by 40 cycles of amplification. Each cycle consisted of a denaturation step (15 seconds at 95 °C) and an annealing/extension step (1 min at 60 °C). Expression levels were normalized to β-actin and data were analyzed by SDS 2.1 software (Applied Biosystems, Foster City, CA).

Microarray analysis

Briefly, 0.5 μg of total RNA was isolated using Paxgene whole blood purification kits or TRIzol® reagent. Oligonucleotide microarray analysis was performed using Affymetrix two-cycle cRNA synthesis and IVT kits according to the manufacturer's protocols (Affymetrix, Santa Clara, CA). cRNA samples (20 μg) were labelled and hybridized to Affymetrix GeneChip Canine Genome 2.0 Arrays to monitor the gene expression of over 18,000 *Canis familiaris* mRNA/EST-based transcripts and over 20,000 non-redundant predicted genes. As described earlier, canine arrays were used following the observation of high levels of homology between canine and ferret nucleotide sequences (average of 89% identity) (Cameron et al., 2008; Rowe et al., 2010). Supplementary Table 1 demonstrates the amino acid identity of genes in this study compared to available orthologues of human and mouse. The arrays were scanned using an Affymetrix GCS3000 7G system according to standard Affymetrix protocols. Probe-level analysis was performed using Probe Logarithmic Error Intensity Estimate (PLIER). The raw intensity values for each individual target on the Affymetrix chips were pre-processed with variance stabilization, $\log_2$-transformation and were then normalized against the time zero datasets with ArrayAssist V 5.5.1 (Stratagene, USA). Student's *t*-tests or EDGE time course differential expression analysis (Storey et al., 2005) were performed with Benjamini–Hochberg false discovery rate (FDR) correction. Genes with a significant difference were selected for agglomerative hierarchical clustering with Pearson distance metrics and average linkage distance measurements between clusters using GeneLinker Platinum V 4.6.1 (Improved Outcomes Software, Kingston, Canada). Ingenuity Pathway Analysis 5.0 software (Ingenuity Systems Inc., Redwood City, CA) was used to annotate and organize the gene expression data into networks and pathways. Pathways and functional categories were considered as over-represented when Fisher's exact test *P* value was ≤ 0.05. Datasets are publicly available at the NCBI's Gene Expression Omnibus (http://www.ncbi.nlm.nih.gov/geo) accession number GSE22581.

Statistical analysis

T tests or EDGE analyses were used for statistical analysis considering a biological filter of 1.5 fold change compared to controls and a *P* value of ≤ 0.05 as significant.

Supplementary materials related to this article can be found online at doi:10.1016/j.virol.2010.10.002.

Acknowledgments

We are indebted to Nikki Kelvin for her editing and critical review of this manuscript. We also would like to thank Lixia Guo and Zujiang Li for their assistance in cloning of the ferret genes. This project was supported by funding from Li Ka Shing Foundation, China; NIH/NIAID Contract No. NOI-AI-30063C11; Southern Research Institute, Contract No. NOI-AI-30067 Task Order No.02; and the Canadian Institute of Health Research No. CIHR-200904PAP-203553-PAM-ADHD-48072.

References

Barclay, J.L., Anderson, S.T., Waters, M.J., Curlewis, J.D., 2007. Regulation of suppressor of cytokine signaling 3 (SOC3) by growth hormone in pro-B cells. Mol. Endocrinol. 21, 2503–2515.

Bonnevie-Nielsen, V., Field, L.L., Lu, S., Zheng, D.J., Li, M., Martensen, P.M., Nielsen, T.B., Beck-Nielsen, H., Lau, Y.L., Pociot, F., 2005. Variation in antiviral 2', 5'-oligoadenylate synthetase (2'5'AS) enzyme activity is controlled by a single-nucleotide polymorphism at a splice-acceptor site in the OAS1 gene. Am. J. Hum. Genet. 76, 623–633.

Bosinger, S.E., Li, Q., Gordon, S.N., Klatt, N.R., Duan, L., Xu, L., Francella, N., Sidahmed, A., Smith, A.J., Cramer, E.M., Zeng, M., Masopust, D., Carlis, J.V., Ran, L., Vanderford, T.H., Paiardini, M., Isett, R.B., Baldwin, D.A., Else, J.G., Staprans, S.I., Silvestri, G., Haase, A.T., Kelvin, D.J., 2009. Global genomic analysis reveals rapid control of a robust innate response in SIV-infected sooty mangabeys. J. Clin. Invest. 119 (12), 3556–3572.

Cameron, M.J., Ran, L., Xu, L., Danesh, A., Bermejo-Martin, J.F., Cameron, C.M., Muller, M.P., Gold, W.L., Richardson, S.E., Poutanen, S.M., Willey, B.M., Devries, M.E., Fang, Y., Seneviratne, C., Bosinger, S.E., Persad, D., Wilkinson, P., Greller, L.D., Somogyi, R., Humar, A., Keshavjee, S., Louie, M., Loeb, M.B., Brunton, J., McGeer, A.J., Kelvin, D.J., 2007. Interferon-mediated immunopathological events are associated with atypical innate and adaptive immune responses in patients with severe acute respiratory syndrome. J. Virol. 81, 8692–8706.

Cameron, C.M., Cameron, M.J., Bermejo-Martin, J.F., Ran, L., Xu, L., Turner, P.V., Ran, R., Danesh, A., Fang, Y., Chan, P.K., Mytle, N., Sullivan, T.J., Collins, T.L., Johnson, M.G., Medina, J.C., Rowe, T., Kelvin, D.J., 2008. Gene expression analysis of host innate immune responses during Lethal H5N1 infection in ferrets. J. Virol. 82, 11308–11317.

Chelbi-Alix, M.K., Wietzerbin, J., 2007. Interferon, a growing cytokine family: 50 years of interferon research. Biochimie 89, 713–718.

Chevaliez, S., Pawlotsky, J.M., 2007. Interferon-based therapy of hepatitis C. Adv. Drug Deliv. Rev. 59, 1222–1241.

Chu, Y.K., Ali, G.D., Jia, F., Li, Q., Kelvin, D., Couch, R.C., Harrod, K.S., Hutt, J.A., Cameron, C., Weiss, S.R., Jonsson, C.B., 2008. The SARS-CoV ferret model in an infection-challenge study. Virology 374, 151–163.

Corssmit, E.P., Heijligenberg, R., Hack, C.E., Endert, E., Sauerwein, H.P., Romijn, J.A., 1997. Effects of interferon-alpha (IFN-alpha) administration on leucocytes in healthy humans. Clin. Exp. Immunol. 107 (2), 359–363.

Danesh, A., Seneviratne, C., Cameron, C.M., Banner, D., Devries, M.E., Kelvin, A.A., Xu, L., Ran, L., Bosinger, S.E., Rowe, T., Czub, M., Jonsson, C.B., Cameron, M.J., Kelvin, D.J., 2008. Cloning, expression and characterization of ferret CXCL10. Mol. Immunol. 45, 1288–1297.

Dawood, F.S., Jain, S., Finelli, L., Shaw, M.W., Lindstrom, S., Garten, R.J., Gubareva, L.V., Xu, X., Bridges, C.B., Uyeki, T.M., 2009. Emergence of a novel swine-origin influenza A (H1N1) virus in humans. N. Engl. J. Med. 360, 2605–2615.

Dushoff, J., Plotkin, J.B., Viboud, C., Earn, D.J., Simonsen, L., 2006. Mortality due to influenza in the United States—an annualized regression approach using multiple-cause mortality data. Am. J. Epidemiol. 163, 181–187.

Fang, Y., Rowe, T., Leon, A.J., Banner, D., Danesh, A., Xu, L., Ran, L., Bosinger, S.E., Guan, Y., Chen, H., Cameron, C.C., Cameron, M.J., Kelvin, D.J., 2010. Molecular characterization of in vivo adjuvant activity in influenza-vaccinated ferrets. J. Virol. 84, 8369–8388.

Gharavi, N.M., Alva, J.A., Mouillesseaux, K.P., Lai, C., Yeh, M., Yeung, W., Johnson, J., Szeto, W.L., Hong, L., Fishbein, M., Wei, L., Pfeffer, L.M., Berliner, J.A., 2007. Role of the Jak/STAT pathway in the regulation of interleukin-8 transcription by oxidized phospholipids in vitro and in atherosclerosis in vivo. J. Biol. Chem. 282, 31460–31468.

Haagmans, B.L., Kuiken, T., Martina, B.E., Fouchier, R.A., Rimmelzwaan, G.F., Van Amerongen, G., van Riel, D., de Jong, T., Itamura, S., Chan, K.H., Tashiro, M., Osterhaus, A.D., 2004. Pegylated interferon-alpha protects type 1 pneumocytes against SARS coronavirus infection in macaques. Nat. Med. 10, 290–293.

Haller, O., Staeheli, P., Kochs, G., 2007. Interferon-induced Mx proteins in antiviral host defense. Biochimie 89, 812–818.

Hull, R.B., Loosli, C.G., 1951. Adrenocorticotrophic hormone (ACTH) in the treatment of experimental air-borne influenza virus type A infection in the ferret. J. Lab. Clin. Med. 37, 603–614.

Kolling, U.K., Hansen, F., Braun, J., Rink, L., Katus, H.A., Dalhoff, K., 2001. Leucocyte response and anti-inflammatory cytokines in community acquired pneumonia. Thorax 56, 121–125.

Li, H., Gade, P., Xiao, W., Kalvakolanu, D.V., 2007. The interferon signaling network and transcription factor C/EBP-beta. Cell. Mol. Immunol. 4, 407–418.

Loutfy, M.R., Blatt, L.M., Siminovitch, K.A., Ward, S., Wolff, B., Lho, H., Pham, D.H., Deif, H., LaMere, E.A., Chang, M., Kain, K.C., Farcas, G.A., Ferguson, P., Latchford, M., Levy, G., Dennis, J.W., Lai, E.K., Fish, E.N., 2003. Interferon alfacon-1 plus corticosteroids in severe acute respiratory syndrome: a preliminary study. JAMA 290, 3222–3228.

Marijanovic, Z., Ragimbeau, J., van der, H.J., Uze, G., Pellegrini, S., 2007. Comparable potency of IFNalpha2 and IFNbeta on immediate JAK/STAT activation but differential down-regulation of IFNAR2. Biochem. J. 407, 141–151.

Martina, B.E., Haagmans, B.L., Kuiken, T., Fouchier, R.A., Rimmelzwaan, G.F., Van Amerongen, G., Peiris, J.S., Lim, W., Osterhaus, A.D., 2003. Virology: SARS virus infection of cats and ferrets. Nature 425, 915.

Ochi, A., Danesh, A., Seneviratne, C., Banner, D., Devries, M.E., Rowe, T., Xu, L., Ran, L., Czub, M., Bosinger, S.E., Cameron, M.J., Cameron, C.M., Kelvin, D.J., 2008. Cloning, expression and immunoassay detection of ferret IFN-gamma. Dev. Comp. Immunol. 32, 890–897.

Okumura, A., Lu, G., Pitha-Rowe, I., Pitha, P.M., 2006. Innate antiviral response targets HIV-1 release by the induction of ubiquitin-like protein ISG15. Proc. Natl. Acad. Sci. U. S. A. 103, 1440–1445.

Rowe, T., Leon, A.J., Crevar, C.J., Carter, D.M., Xu, L., Ran, L., Fang, Y., Cameron, C.M., Cameron, M.J., Banner, D., Ng, D.C., Ran, R., Weirback, H.K., Wiley, C.A., Kelvin, D.J., Ross, T.M., 2010. Modeling host responses in ferrets during A/California/07/2009 influenza infection. Virology 401, 257–265.

Shapira, S.D., Gat-Viks, I., Shum, B.O., Dricot, A., de Grace, M.M., Wu, L., Gupta, P.B., Hao, T., Silver, S.J., Root, D.E., Hill, D.E., Regev, A., Hacohen, N., 2009. A physical and regulatory map of host–influenza interactions reveals pathways in H1N1 infection. Cell 139 (7), 1255–1267.

Staal, F.J., Luis, T.C., Tiemessen, M.M., 2008. WNT signalling in the immune system: WNT is spreading its wings. Nat. Rev. Immunol. 8 (8), 581–593.

Storey, J.D., Xiao, W., Leek, J.T., Tompkins, R.G., Davis, R.W., 2005. Significance analysis of time course microarray experiments. Proc. Natl. Acad. Sci. U. S. A. 102 (36), 12837–12842.

Takaoka, A., Yanai, H., 2006. Interferon signalling network in innate defence. Cell. Microbiol. 8, 907–922.

Thompson, W.W., Shay, D.K., Weintraub, E., Brammer, L., Cox, N., Anderson, L.J., Fukuda, K., 2003. Mortality associated with influenza and respiratory syncytial virus in the United States. JAMA 289, 179–186.

Uddin, S., Platanias, L.C., 2004. Mechanisms of type-I interferon signal transduction. J. Biochem. Mol. Biol. 37, 635–641.

Weiss, R.A., McMichael, A.J., 2004. Social and environmental risk factors in the emergence of infectious diseases. Nat. Med. 10, S70–S76.